

Redistribution of global precipitation observed in the El Niño events by using remote sensing

L.N. Vasiliev

Institute of Geography Russian Academy of Sciences, Moscow, Russia

Keywords: precipitation anomaly, dynamical structure, density of states

ABSTRACT: El Niño is a disruption of the ocean-atmosphere system in the tropical Pacific having important consequences for weather around the globe. The paper has two main objectives. The first is to understand the relationship between the centre of gravity of global precipitation and its spatial structure. The second to investigate the interaction of global precipitation with the extreme event such as El Niño. The 6-year duration from October 1996 through July 2002 is long enough to capture several annual cycles, as well as some aspects of El Niño-related variability. The dynamical properties of precipitation structure were evaluated with the introduction of some characteristics. The seasonal and interannual variability in precipitation and large-scale mass redistribution between the Northern and Southern Hemispheres are described by the trajectory of the centre of gravity of precipitation. The dynamic structure is described by the vibrational density of states, which is characterized by the spectral dimension. The use of One-Degree Daily precipitation data from satellite remote sensing made it possible to experimentally estimate the size and location of precipitation anomalies due to the global atmospheric manifestation of El Niño. In anomalous areas the volume of precipitation grows and drops by the factor of 2 and 2.5 respectively. The increase of the total amount of global precipitation during El Niño is accompanied by its simultaneous redistribution in the regions far removed from the tropical Pacific.

1 INTRODUCTION

El Niño is a disruption of the ocean-atmosphere system in the tropical Pacific having important consequences for weather around the globe. El Niño is characterized by a large scale weakening of the trade winds and warming of surface layers in the eastern and central equatorial Pacific. The phenomenon occurs irregularly at intervals from 2 to 7 years although the average is about one every 3-4 years. Usually it lasts 12-18 months and is accompanied by swings in the Southern Oscillation Index. The process is named El Niño Southern Oscillation (ENSO) (Hayes et al 1991, McPhaden 1993, Philander 1990). During the El Niño event when trade winds are getting weaker warm water masses from the West Pacific shift eastwards. The sea surface temperature of the central and the eastern part of the Pacific varies by up to about 3° to 4°C with associated changes in the winds direction and rainfall pattern. El Niño phenomenon implications manifest themselves most drastically near the equator. Among these consequences are increased rainfalls across the southern areas of the US and Peru, which has caused destruc-

tive flooding and draught in the West Pacific, sometimes associated with devastating brush fires in Australia. It is useful to remember that El Niño is a normal part of the climate system of the Pacific. The origin of El Niño remains unexplained. Perhaps it can be thought of as an example of self-organized criticality in the environment which would help explain an avalanche-like dynamics originated in the ocean-atmosphere system, the latter being in the condition of interrupted equilibrium. Most investigations deal with regional implications of El Niño manifestations (NOAA, web site). However, the eastward displacement of the atmospheric heat results in large changes in the global atmosphere circulation, which in turn force changes in weather in regions far removed from the tropical Pacific. Starting in October 1996 the Global Precipitation Climatology Project (GPCP) produces globally complete daily estimates of precipitation on a 1°x1° lat/long grid from currently available observation data (Huffman et al 2001). Despite much progress achieved recently in El Niño observations, there are several unanswered questions associated with the redistribution of global precipitation. One of the key questions is how precipitation behaves in the pres-

ence of the El Niño. The results of the research are offered in the paper.

2 DYNAMIC PROPERTIES OF THE SPATIAL STRUCTURE OF GLOBAL PRECIPITATION

The One-Degree Daily (1DD) precipitation data set is the first approach to estimating global daily precipitation at $1^\circ \times 1^\circ$ scale completely from observational systems (GEOS, SSM/I, TOVS). This data set was derived as part of the Global Precipitation Climatology Project (GPCP). All available 1DD data belong to the period October 1996 through August 2002.

Global precipitation forms in space and time a 3D infinite cluster. The cluster covers in space and time about 48 percent of the entire volume. It means that on the average 48 percent of the Earth's surface is the subject of every day precipitation Vasiliev (2002). The fractal structure of global precipitation is characterized by dynamic properties, which determine their everyday redistribution and the relationship between the total amount of precipitation in the Southern and Northern Hemispheres. The latter is associated with the fact that twice a year the Sun crosses the equator. The El Niño effect on the behaviour of global precipitation is revealed by determining their centre of gravity. If precipitation had been uniformly distributed all over the surface of the Earth, the centre of gravity would have been in the centre of the Earth. The actual distribution brings about the shift of the centre of gravity, and its trajectory characterizes dynamic properties of the space-time structure of precipitation.

If the centre of gravity of precipitation is specified as a 3D Cartesian coordinate X, Y, Z from the origin in the centre of the Earth, then its projection on the Earth's surface will be given in terms of latitude and longitude. A latitudinal movement of the centre of gravity of global precipitation, which is a function of $Z(t)$ from October 1 1996 through July 31 2002, is shown in Figure 1a. The latitudinal seasonal cycle of the center of gravity is naturally associated with the difference between diurnal precipitation in the Northern and Southern Hemispheres (Fig. 1b). The ratio of precipitation in both hemispheres varies within $[3, 0.33]$. The sine function fits well both data. It shows that the trajectory of the center of gravity varies in latitude within $[-5^\circ\text{N}, 5^\circ\text{S}]$ in accordance with the Sun crossing the equator twice a year. The sinusoidally varying trajectories of the Sun and the center of gravity are out of phase, the phase difference being about 3 months.

Let us consider a model atmosphere that has a uniform temperature and rotates at the same rate as the Earth. If one starts to heat the air at a low level

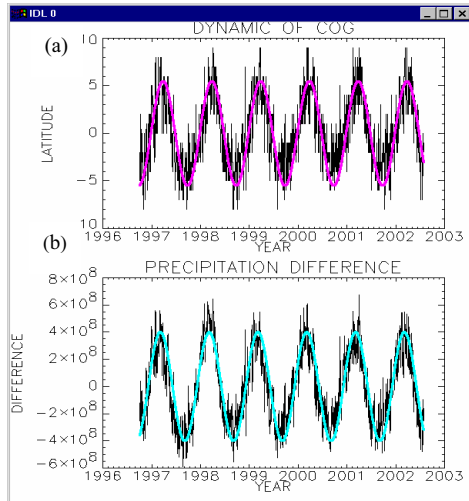


Figure 1. (a) The usual latitudinal seasonal cycle of the center of gravity of global precipitation. A sinusoidal fit function to the observed center of gravity shows an annual cycle with random fluctuations. (b) The temporal variation in the difference between daily precipitation in the Northern and Southern Hemispheres. Proportion between the sums of precipitation varies in the interval $[3.0, 0.33]$. Units are $\times 10^{12}$ kg.

on the summer side of the equator, the local temperature will rise and the air column will expand mainly in the vertical direction. This process will create, at the upper levels, a relatively high-pressure belt located over the thermal equator. Next, the north-south pressure gradient will force the equatorial air at all longitudes to move toward the low-pressure zone, mainly into the winter hemisphere, where initially vertical contraction occurs as a result of radiative cooling. The air will then slowly start to sink over a wide region in the winter hemisphere and will return to the equator at low levels. The cycle will be closed finally by a rise of the air after it has arrived in the vicinity of the thermal equator. A simple cellular circulation would be completely symmetrical with respect to the earth's axis of rotation. Despite the oversimplifying, the dynamics of the centre of gravity of global precipitation ensures an excellent agreement between the model of atmospheric convection and observations.

X, Y , specifies the location of the centre of gravity of precipitation in the equatorial plane. Its projection on the equator is specified by a longitude. The X, Y scatter plot (Fig. 2) shows that the centre of gravity of precipitation stays steadily on the interface of the Eastern and Western Hemispheres. It implies persistently higher precipitation in the hemisphere located within $[90^\circ\text{W}, 180^\circ, 90^\circ\text{E}]$. The trajectory of the centre of gravity along the longitude is shown on Figure 3. In normal conditions the projection of the centre of gravity oscillates near 160°E . However, during the El Niño period since

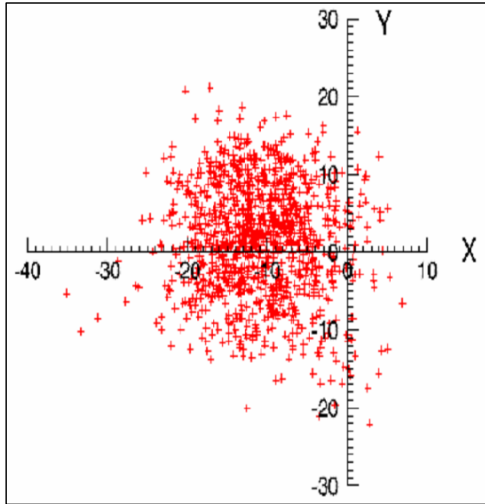


Figure 2. Scatter plot of the centre of gravity of global precipitation in the equatorial cross-section. The location of centres of gravity is shifted from the Greenwich direction.

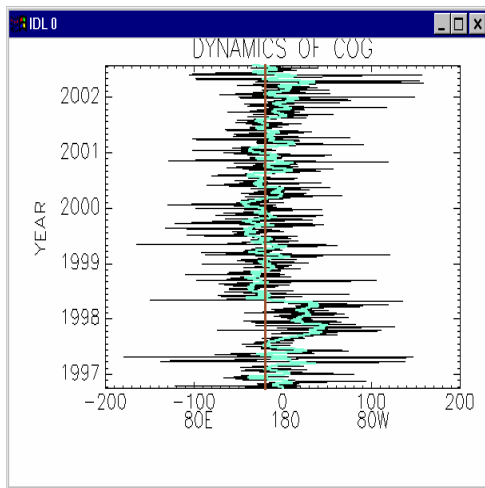


Figure 3. Longitudinal trajectory of the centre of gravity of global precipitation. The trajectory oscillates along the 160° E meridian. The plot illustrates the original values and values smoothed with width a 30 days moving average (heavy line). Large-scale mass redistribution in precipitation drifts out the center of gravity eastwards to 149° W.

September 1997 to April 1998 precipitation redistribution displaces their gravity centre eastwards to 149°W shifting it along the equator by 5700 km. The trajectory shows that the redistribution of precipitation in the initial and final phases of El Niño behaves differently. Gradual eastward displacement of precipitation begins before a considerable rise of sea

surface temperature and ceases by the abrupt redistribution in the period of cooling. The gravity centre displacement from September 1997 through April 2002 agrees with the anomaly of the sea surface temperature. However, the redistribution of precipitation occurs before the beginning of the SST increase and this becomes evident from the displacement of the centre of gravity already by the end of 1996 and in the case of weaker El Niño from October 2001 through April 2002.

3 ANOMALIES OF GLOBAL PRECIPITATION

The displacement of the position of the centre of gravity of global precipitation implies its redistribution, but does not dominate the change of the spatial structure and the location of anomalies. Precipitation anomalies are detected from the comparison of the values on a 1°x1° grid accumulated during normal and El Niño condition. The sum of precipitation for all 1°x1° cells during the El Niño period from October 1997 to May 1998 was compared with five sums calculated for the equivalent time intervals in 1996 – 2002. The result of comparison is shown on Figure 4

Regions of increasing and decreasing precipitation do not form a single compact group, rather they are scattered all over the globe. Anomalous behaviour in each cell means that the value of the sum of precipitation during El Niño significantly greater or less than all the values (five) for normal years. An important feature of Figure 4 is that the total amount of precipitation during seven-El Niño months increases by a factor of 1.17 ± 0.04 . The latter, however, requires further explanation.

4 DENSITY OF STATES OF GLOBAL PRECIPITATION

The fractal space-time structure of precipitation is characterized by dynamic scaling (Vasiliev 2003). Scaling has proven to be a very valuable tool for obtaining insight into dynamical properties of space-time precipitation. The idea of vibration on a percolating network may be used to interpret a space-time series of global precipitation. We consider a rainfall in the space-time coordinate system X, Y, t . If in each 1°x1° cell the start of precipitation, t_s , and its end, t_e , are recorded, the entire time axis would be subdivided into intervals

$$\Delta t = \begin{cases} t_s - t_e, & \text{with precipitation} \\ t_e - t_s, & \text{without precipitation} \end{cases}$$

The set of Δt all over the globe permits the behaviour of events to be characterized in the frequency domain, $\omega = \Delta t^{-1}$, which is measured in 1/day.

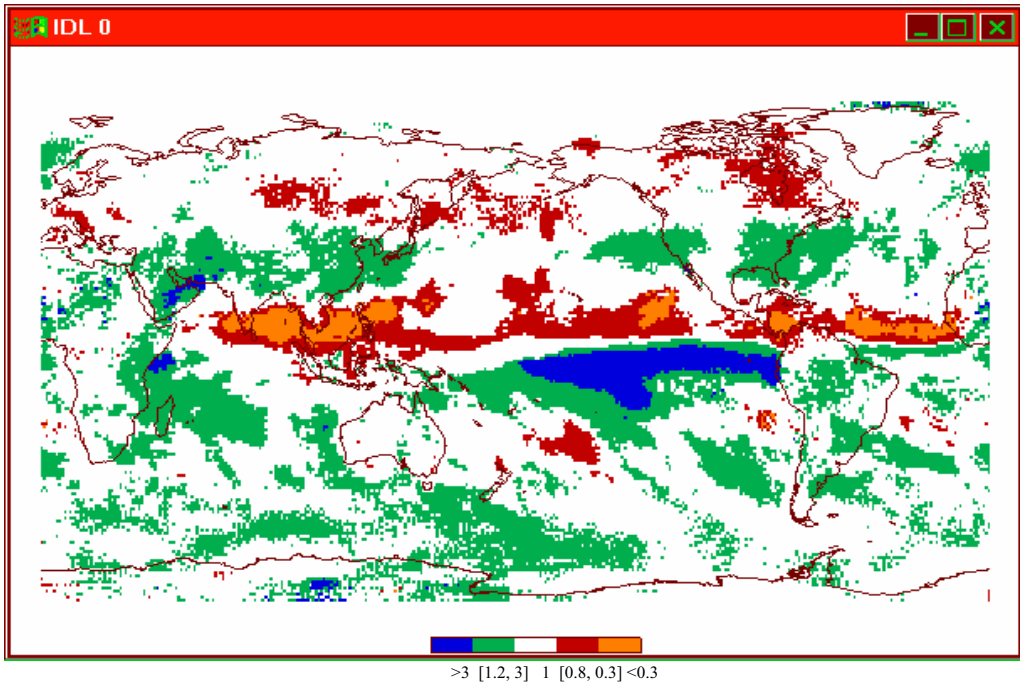


Figure 4. Observed precipitation anomalies during El Niño in 1997 – 1998. The anomalies show how much the sum of precipitation during seven months El Niño differs from the usual value for the same months in 1996 – 1997, 1998 – 2002. The anomalies are presented in two terms: increase and decrease of precipitation. The ratios of the sums of precipitation during El Niño condition to normal condition have ranged for the increase: [1.2, 3.0] and greater than 3.0. For the decrease: [0.80, 0.33] and less than 0.33. The anomalies significantly greater than the norms are shown in green and blue and anomalies less than the norms are shown in red and orange.

The vibrational density of states DOS, $D(\omega)$, is defined by $D(\omega) \propto \omega^{d_s}$, where d_s is the spectral dimension (Nakayama, Yakubo and Orbach 1997). The DOS of precipitation are computed for the all normal years and El Niño condition for the area with an increase/decrease of precipitation with results exhibited in Figure 5. The plot shows that there exist two characteristic frequencies ω for spatial and temporal variability of precipitation events and the DOS is characterized by two regimes. The region in the vicinity of ω_c is the crossover region. The crossover ω_c can be thought of as dimensionality change corresponding to the transition from the air mass shower regime to rainfalls produced by organized systems like tropical cyclones. For normal condition

$$D(\omega) = \begin{cases} \omega^{1.55}, & \omega > \omega_c \\ \omega^{2.95}, & \omega < \omega_c \end{cases}$$

and for the El Niño

$$D(\omega) = \begin{cases} \omega^{1.55}, & \omega > \omega_c \\ \omega^{2.42}, & \omega < \omega_c \end{cases}$$

It should be emphasized that the crossover frequency ω_c radically depends on the spatial and temporal resolution. For the above-mentioned data set the crossover frequency $\omega_c = 1/(9 \text{ days})$, hence one should be careful to interpret the meaning of this frequency. For higher resolution the crossover will shift to the lower frequency region, that is, to shorter time intervals Δt .

The vibrational density of states and spectral dimension d_s explain the large-scale precipitation redistribution when they had been increasing. Figure 5 shows a noticeable change in frequency dependence of the DOS of global precipitation during El Niño. In the case of $\omega > \omega_c$ (short time intervals) the overall amount of events decreases. For the case $\omega < \omega_c$ (long time intervals) the number of events increases resulting in an increase of precipitation. In the anomalies with decreasing precipitation their behaviour changes to opposite, which is a slight increase of the number of events, mainly due to short-term precipitation and a significant increase of long intervals without rainfall.

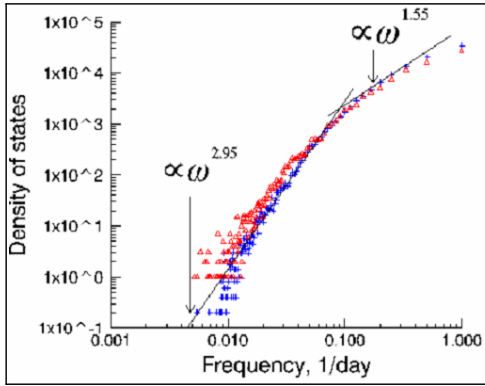


Figure 5. The density of states $D(\omega)$ differences between precipitation under normal condition (+) and El Niño (triangle) in the anomalies with increasing of precipitation (shown on Figure 4). Power law dependence in the vibrational density of states $D(\omega)$ is shown for normal condition in black line.

5 DISCUSSION

To fully understand the change in the behaviour of global precipitation, the dynamics of anomalies should be estimated. In other words, the rate of accumulation of precipitation in both negative and positive anomalies should be explained. Figure 6 presents the difference between two cumulative sums of precipitation for both anomalies. These cumulative sums calculated over a 200-day period in the anomalies with precipitation increase/decrease are compared with cumulative sums taken over a similar period for five normal years. Five cumulative sums for a normal condition are very similar but much different from El Niño condition. In the region with a deficit in precipitation they cease 1.5 to 2 months after the El Niño effect started. Within seven months precipitation anomalies increased by a factor of two and decreased from the normal amount till 0.4.

6 CONCLUSIONS

Despite much progress achieved recently in the El Niño observation, there are still important unanswered questions associated with the redistribution of precipitation. One of the key questions is how does precipitation behave in the presence of the El Niño? Better understanding of global precipitation redistribution has been achieved due to the development of new theoretical concept concerning their dynamic structure. The dynamical properties of the precipitation structure were evaluated with the introduction of some characteristics. The seasonal and interannual variability in precipitation and large-scale

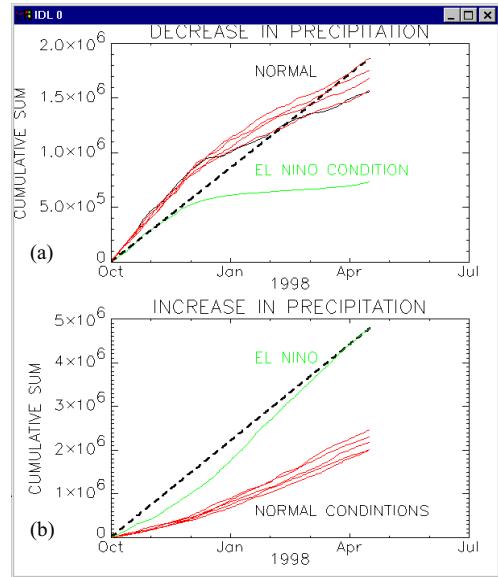


Figure 6. Redistribution of the cumulative sums of precipitation in the anomalies during El Niño. Differences between the cumulative sums under normal condition for five years before and after 1997 – 1998 El Niño and El Niño condition. (a) Decrease of precipitation, (b) increase of precipitation. The dash line is a cumulative sum for daily uniform precipitation rate.

mass redistribution between the Northern and Southern Hemispheres are described by the trajectory of the centre of gravity of precipitation. The dynamic structure is described by the vibrational density of states, which is characterized by the spectral dimension. The use of One-Degree Daily precipitation data from satellite remote sensing made it possible to experimentally estimate the size and location of precipitation anomalies due to global atmospheric manifestations of El Niño. The increase of the total amount of global precipitation during El Niño is accompanied by their simultaneous redistribution in the regions far removed from the tropical Pacific. In anomalous areas the volume of precipitation grows and drops by the factor of 2 and 2.5, respectively. In the area of a negative anomaly rainfall is very sparse 1.5 to 2 months after the commencement of El Niño. A new approach to analysis of satellite remote sensing 1DD data and the results of precipitation redistribution provide the theoretical and experimental basis for the ability to predict both the simultaneous and lagged effects of El Niño occurrences on the seasonal climate of the regions of the world.

ACKNOWLEDGEMENTS

The 1DD data were provided by the NASA/Goddard Space Flight Center's Laboratory for Atmospheres, which develops and computes the 1DD as a contribution to the GEWEX Global Precipitation Climatology Project.

REFERENCES

- Hayes, S.P., Mangum, L.J., Picaut, J., Sumi, A., Takeuchi, K. 1991. TOGA-TAO: A moored array for real-time measurements in the tropical Pacific Ocean. *Bull. Am. Meteorol. Soc.*, 72, 339-347.
- Huffman, G.J., Adler, R.F. et al. 2001. Global Precipitation at one-degree daily resolution from multi-satellite observations. *Journal of Hydrometeorology*, 2, 36-50.
- Nakayama, T., Yakubo, K., Orbach, R.L. 1994. Dynamical properties of fractal networks: Scaling, numerical simulations, and physical realizations. *Reviews of Modern Physics* Vol. 66 (No 2): 381-443.
- McPhaden, M.J., 1993. TOGA-TAO and the 1991-93 El Niño-Southern Oscillation event. *Oceanography*, 6, 36-44.
- NOAA/PMEL/TAO El Niño Impacts web site.
- Philander, S.G.H., 1990. El Niño, La Niña and the Southern Oscillation. Academic Press, San Diego, CA, 289 pp.
- Vasiliev, L. 2002. Spatio-temporal pattern formation in rainfall from remote sensing observations. In G. Begni (ed.). *Observing our environment from space*. Balkema, Rotterdam, 159-165.
- Vasiliev, L. 2003. Dynamic scaling in the environment and remote sensing observation. In T. Benes (ed.). *Geoinformation for European-wide Integration*. Millpress, Rotterdam, 65-69.